RECURSIVE VERSIONS OF THE LEVENBERG-MARQUARDT REASSIGNED SPECTROGRAM AND OF THE SYNCHROSQUEEZED STFT

Dominique Fourer[1], *François Auger*[1], *Patrick Flandrin*[2]

[1] LUNAM University, IREENA, Saint-Nazaire, France

[2] Laboratoire de Physique de l'École Normale Supérieure de Lyon, CNRS and Université de Lyon, France

dominique.fourer@univ-nantes.fr, francois.auger@univ-nantes.fr, patrick.flandrin@ens-lyon.fr

ABSTRACT

In this paper, we first present a recursive implementation of a recently proposed reassignment process called the Levenberg-Marquardt reassignment, which allows a user to adjust the slimness of the signal components localization in the time-frequency plane. Thanks to a generalization of the signal reconstruction formula, we also present a recursive implementation of the synchrosqueezed short-time Fourier transform. This approach paves the way for a real-time computation of a reversible and adjustable almost-ideal time-frequency representation.

***Index Terms*—** time-frequency analysis, reassignment, synchrosqueezing, short-time Fourier transform, recursive filtering.

1. INTRODUCTION

Time-frequency analysis aims at expanding a signal into a set of non-stationary components and can be performed using the well-known Short-Time Fourier Transform (STFT). However, this tool suffers from a poor energy localization in the time-frequency plane. A possible improvement was proposed by the reassignment method, introduced by Kodera *et al.*[1] and generalized by Auger and Flandrin to any time-frequency distribution of the Cohen and affine classes in [2]. Recently, Auger *et al.*[3] proposed an extension of this method inspired by the Levenberg-Marquardt algorithm, that uses the second-order derivatives of the phase of the STFT for the time-frequency localization of the signal components to be weaker or stronger than with the classical reassignment. But although an efficient Time Frequency Representation (TFR), the reassigned spectrogram is not directly invertible. To this aim, the synchrosqueezing was proposed, initially introduced for the Continuous Wavelet Transform (CWT) [4] and later extended to the STFT [5, 6, 7, 8]. But all these approaches require the computation of several STFTs using non-causal windows which prevent their use in real-time applications. This problem can efficiently be solved by considering a specific case of the STFT that can be recursively computed thanks to the use of a causal window function as in [9]. In the present work, the first- and second-order derivatives of the phase of the STFT are derived for this particular case and lead to a practical real-time implementation of both the classical and the Levenberg-Marquardt reassigned spectrograms, and to the first (to our knowledge) real-time implementation of a synchrosqueezed STFT. This paper is organized as follows: in section 2, the STFT is related to convolution products, to which reassignment and synchrosqueezing are applied. In section 3, a particular analysis window is considered to allow its implementation by causal recursive filters. Experimental results obtained with these approaches are presented in section 4 and finally discussed with possible extensions in section 5.

This research was supported by the French ANR ASTRES project (ANR-13-BS03-0002-01).

2. FILTER-BASED STFT, ITS REASSIGNMENT AND SYNCHROSQUEEZING

The STFT $F_x^h(t,\omega) = M_x^h(t,\omega)\,\mathrm{e}^{j\Phi_x^h(t,\omega)}$, as defined for example in [3], can be related to the linear convolution product between the analyzed signal x and the complex valued impulse response of a bandpass filter centered on ω, $g(t,\omega) = h(t)\,\mathrm{e}^{j\omega t}$, $h(t)$ being a real-valued analysis window:

$$y_x^g(t,\omega) = \int_{-\infty}^{+\infty} g(\tau,\omega)x(t-\tau)\,d\tau = |y_x^g(t,\omega)|\,\mathrm{e}^{j\Psi_x^g(t,\omega)} \quad (1)$$

$$= F_x^h(t,\omega)\,\mathrm{e}^{j\omega t} = M_x^h(t,\omega)\,\mathrm{e}^{j(\Phi_x^h(t,\omega)+\omega t)} \quad (2)$$

This implies that its magnitude M and its phase Φ can be deduced from the phase and magnitude of $y_x^g(t,\omega)$ by $M_x^h(t,\omega) = |y_x^g(t,\omega)|$ and $\Phi_x^h(t,\omega) = \Psi_x^g(t,\omega) - \omega t$.

2.1. Rewording the classical reassignment

The reassignment method, introduced in [1] and generalized by Auger and Flandrin in [2], aims at sharpening a TFR. This improved localization of the signal components is obtained by reassigning the values of an energy distribution to coordinates that are closer to the real support of the analyzed signal.

According to [1, 2], the reassignment operators of the spectrogram can be related to the phase of the STFT and thus can be reformulated using the phase of $y_x^g(t,\omega)$, denoted Ψ_x^g, as

$$\hat{t}(t,\omega) = -\frac{\partial \Phi_x^h}{\partial \omega}(t,\omega) = t - \frac{\partial \Psi_x^g}{\partial \omega}(t,\omega), \quad (3)$$

$$\hat{\omega}(t,\omega) = \omega + \frac{\partial \Phi_x^h}{\partial t}(t,\omega) = \frac{\partial \Psi_x^g}{\partial t}(t,\omega). \quad (4)$$

In practice, the partial derivatives of Ψ_x^g can be deduced from convolution products of the signal with particular impulse responses, as will be detailed in section 2.3. Then, the reassigned spectrogram can simply be defined using the reassigned coordinates as $\mathrm{R}_x^h(t,\omega) =$

$$\iint_{\mathbb{R}^2} |y_x^g(t',\omega')|^2 \delta(t-\hat{t}(t',\omega'))\delta(\omega-\hat{\omega}(t',\omega'))\, dt'd\omega', \quad (5)$$

where $\delta(t)$ denotes the Dirac distribution.

2.2. Rewording the Levenberg-Marquardt reassignment

Reflection on reassignment was continued, and by analogy with the Levenberg-Marquardt root finding algorithm, new reassignment operators were derived [3] which allow to adjust the energy localization in the time-frequency plane through a damping parameter μ, which could be locally matched to the signal content by or by a noise only/signal+noise binary detector [10, 11]. These new reassignment operators can also be expressed as a function of the phase Ψ_x^g of y_x^g:

$$\begin{pmatrix}\tilde{t}(t,\omega)\\ \tilde{\omega}(t,\omega)\end{pmatrix} = \begin{pmatrix} t\\ \omega\end{pmatrix} - \left(\nabla^t R_x^h(t,\omega) + \mu I_2\right)^{-1} R_x^h(t,\omega) \quad (6)$$

$$R_x^h(t,\omega) = \begin{pmatrix} t-\hat{t}(t,\omega)\\ \omega-\hat{\omega}(t,\omega)\end{pmatrix} = \begin{pmatrix} \frac{\partial \Psi_x^g}{\partial \omega}(t,\omega)\\ \omega - \frac{\partial \Psi_x^g}{\partial t}(t,\omega)\end{pmatrix} \quad (7)$$

$$\begin{aligned}\nabla^t R_x^h(t,\omega) &= \begin{pmatrix} \frac{\partial R_x^h}{\partial t}(t,\omega) & \frac{\partial R_x^h}{\partial \omega}(t,\omega)\end{pmatrix}\\ &= \begin{pmatrix} \frac{\partial^2 \Psi_x^g}{\partial t\partial \omega}(t,\omega) & \frac{\partial^2 \Psi_x^g}{\partial \omega^2}(t,\omega)\\ -\frac{\partial^2 \Psi_x^g}{\partial t^2}(t,\omega) & 1-\frac{\partial^2 \Psi_x^g}{\partial t\partial \omega}(t,\omega)\end{pmatrix}\end{aligned} \quad (8)$$

where I_2 is the 2×2 identity matrix. As a result, the Levenberg-Marquardt reassigned spectrogram can be obtained by replacing $(\hat{t},\hat{\omega})$ by $(\tilde{t},\tilde{\omega})$ in Eq. (5).

2.3. Rewording the partial derivatives of the phase

As detailed in [3, 12], the first- and second-order derivatives of the phase can be computed from STFTs using specific windows. If, unlike [3, 2], the phase Ψ and the impulse response g of the bandpass filters are used instead of Φ and h, these partial derivatives can be computed as

$$\frac{\partial \Psi_x^g}{\partial t}(t,\omega) = \mathrm{Im}\left(\frac{y_x^{\mathcal{D}g}(t,\omega)}{y_x^g(t,\omega)}\right) \quad (9)$$

$$\frac{\partial \Psi_x^g}{\partial \omega}(t,\omega) = \mathrm{Re}\left(\frac{y_x^{\mathcal{T}g}(t,\omega)}{y_x^g(t,\omega)}\right) \quad (10)$$

$$\frac{\partial^2 \Psi_x^g}{\partial t\partial \omega}(t,\omega) = \mathrm{Re}\left(\frac{y_x^{\mathcal{D}\mathcal{T}g}(t,\omega)}{y_x^g(t,\omega)} - \frac{y_x^{\mathcal{D}g}(t,\omega)y_x^{\mathcal{T}g}(t,\omega)}{y_x^g(t,\omega)^2}\right) \quad (11)$$

$$\frac{\partial^2 \Psi_x^g}{\partial t^2}(t,\omega) = \mathrm{Im}\left(\frac{y_x^{\mathcal{D}^2g}(t,\omega)}{y_x^g(t,\omega)} - \left(\frac{y_x^{\mathcal{D}g}(t,\omega)}{y_x^g(t,\omega)}\right)^2\right) \quad (12)$$

$$\frac{\partial^2 \Psi_x^g}{\partial \omega^2}(t,\omega) = -\mathrm{Im}\left(\frac{y_x^{\mathcal{T}^2g}(t,\omega)}{y_x^g(t,\omega)} - \left(\frac{y_x^{\mathcal{T}g}(t,\omega)}{y_x^g(t,\omega)}\right)^2\right) \quad (13)$$

where $\mathrm{Re}(z)$ and $\mathrm{Im}(z)$ are respectively the real and imaginary parts of a complex number z and y_x^g, $y_x^{\mathcal{T}g}$, $y_x^{\mathcal{D}g}$, $y_x^{\mathcal{D}\mathcal{T}g}$, $y_x^{\mathcal{T}^2g}$ and $y_x^{\mathcal{D}^2g}$ are the outputs of the filters using respectively the impulse responses $g(t,\omega)$, $\mathcal{T}g = t\,g(t,\omega)$, $\mathcal{D}g(t,\omega) = \frac{\partial g}{\partial t}(t,\omega)$, $\mathcal{D}\mathcal{T}g(t,\omega) = \frac{\partial}{\partial t}\left(t\,g(t,\omega)\right)$, $\mathcal{T}^2g(t,\omega) = t^2g(t,\omega)$ and $\mathcal{D}^2g(t,\omega) = \frac{\partial^2 g}{\partial t^2}(t,\omega)$.

2.4. Rewording the synchrosqueezed STFT

As defined in Eq. (1), y_x^g admits the following signal reconstruction formula

$$x(t-t_0) = \frac{1}{h(t_0)}\int_{-\infty}^{+\infty} y_x^g(t,\omega)\,\mathrm{e}^{-j\omega t_0}\,\frac{d\omega}{2\pi}, \quad (14)$$

when $\omega \mapsto y_x^g(t,\omega)$ is integrable and when $h(t_0)\neq 0$. These assumptions are supposed to be always verified in the remainder of this paper. This shows that $x(t)$ can be recovered from y_x^g with a time-delay $t_0 \geq 0$. Usually, a symmetric non-causal window h is used and the location of its the maximum is $t_0 = 0$. In some cases, for example when $h(0) = 0$, the best choice of t_0 depends on the window shape and should be chosen close to its maximum, as shown in section 4.

The synchrosqueezing method [4] is an alternative to the reassignment method that provides a sharpened linear time-frequency transform while allowing the signal reconstruction. The synchrosqueezed STFT [6] only uses the frequency coordinate reassignment operator and can be deduced from the synthesis formula (14) as

$$\mathrm{Sy}_x^g(t,\omega) = \int_{\mathbb{R}} y_x^g(t,\omega')\,\mathrm{e}^{-j\omega' t_0}\,\delta\left(\omega - \hat{\omega}(t,\omega')\right)\,d\omega'. \quad (15)$$

Hence, $|\mathrm{Sy}_x^g(t,\omega)|^2$ provides a sharpen TFR and $x(t)$ can be estimated with a time-delay t_0 by

$$\hat{x}(t-t_0) = \frac{1}{h(t_0)}\int_{\mathbb{R}} \mathrm{Sy}_x^g(t,\omega)\,\frac{d\omega}{2\pi}. \quad (16)$$

In practice, each signal component can be recovered individually as proposed in [6] by restricting the integration area to the vicinity of each ridge. Eq. (15) classically uses the frequency reassignment operator defined by Eqs. (4) and (9). We propose to define a Levenberg-Marquardt Synchrosqueezed STFT by replacing $\hat{\omega}$ by $\tilde{\omega}$ in Eq. (15). This new synchrosqueezing process allows to adjust the time-frequency localization of the signal components while allowing signal reconstruction and mode extraction.

3. TOWARDS A RECURSIVE IMPLEMENTATION

As proposed in [9], y_x^g can be recursively implemented if we use for $h(t)$ a causal recursive infinite impulse response filter

$$h_k(t) = \frac{t^{k-1}}{T^k(k-1)!}\,\mathbf{e}^{-t/T}\,U(t), \tag{17}$$

$$g_k(t,\omega) = h_k(t)\,\mathbf{e}^{j\omega t} = \frac{t^{k-1}}{T^k(k-1)!}\,\mathbf{e}^{pt}\,U(t) \tag{18}$$

with $p = -\frac{1}{T} + j\omega$, $k \geq 1$ being the filter order, T the time spread of the window and $U(t)$ the Heaviside step function.

3.1. Discretization

Using the impulse invariance method [13], the filter defined by Eqs. (1) and (18) can be implemented as [9]

$$G_k(z,\omega) = T_s \mathcal{Z}\left\{g_k(t,\omega)\right\} = \frac{\sum_{i=0}^{k-1} b_i z^{-i}}{1+\sum_{i=1}^{k} a_i z^{-i}}, \tag{19}$$

with $b_i = \frac{1}{L^k(k-1)!} B_{k-1,k-i-1}\alpha^i$, $\alpha = \mathbf{e}^{pT_s}$, $L = T/T_s$, $\mathcal{Z}\left\{f(t)\right\} = \sum_{n=0}^{+\infty} f(nT_s) z^{-n}$, $a_i = A_{k,i}\left(-\alpha\right)^i$, T_s being the sampling period. $B_{k,i} = \sum_{j=0}^{i}(-1)^j A_{k+1,j}(i+1-j)^k$ denotes the Eulerian numbers and $A_{k,i} = \begin{pmatrix} k \\ i \end{pmatrix} = \frac{k!}{i!(k-i)!}$ the binomial coefficients. Hence, $y_k[n,m] \approx y_x^{g_k}(nT_s, \frac{2\pi m}{MT_s})$ can be computed from the sampled analyzed signal $x[n]$ by a standard recursive equation

$$y_k[n,m] = \sum_{i=0}^{k-1} b_i\, x[n-i] - \sum_{i=1}^{k} a_i\, y_k[n-i,m] \tag{20}$$

where $n \in \mathbb{Z}$ and $m = 0, 1, ..., M-1$ are respectively the discrete time and frequency indices. The z transform of the other specific impulse responses can be expressed as functions of $G_k(z,\omega)$ at different orders

$$T_s\mathcal{Z}\{\mathcal{T} g_k(t,\omega)\} = kTG_{k+1}(z,\omega) \tag{21}$$

$$T_s\mathcal{Z}\left\{\mathcal{D} g_k(t,\omega)\right\} = \frac{1}{T}G_{k-1}(z,\omega) + pG_k(z,\omega) \tag{22}$$

$$T_s\mathcal{Z}\left\{\mathcal{D}\mathcal{T} g_k(t,\omega)\right\} = k\left(G_k(z,\omega) + pTG_{k+1}(z,\omega)\right) \tag{23}$$

$$T_s\mathcal{Z}\left\{\mathcal{T}^2 g_k(t,\omega)\right\} = k(k+1)T^2 G_{k+2}(z,\omega) \tag{24}$$

$$T_s\mathcal{Z}\left\{\mathcal{D}^2 g_k(t,\omega)\right\} = \frac{1}{T^2}G_{k-2}(z,\omega) + \frac{2p}{T}G_{k-1}(z,\omega) + p^2 G_k(z,\omega). \tag{25}$$

These results hold for any $k \geq 1$ provided that $G_0(z,\omega) = G_{-1}(z,\omega) = 0$. Eqs. (21) and (22) generalize to any value of k some results already presented in [9], while Eqs. (23) to (25) provide the discrete-time linear systems required by the Levenberg-Marquardt reassignment operators.

3.2. Recursive reassignment and synchrosqueezing

The discretization of the reassignment operators given by Eqs. (3), (4), (6), (7) and (8) combined with expressions of the specific windows as functions of $G_k(z,\omega)$ leads to the following expressions of the discrete-time reassigned coordinates [9]

$$\hat{n}[n,m] = n - \mathrm{Round}\left(\mathrm{Re}\left(\frac{T_s^{-1} y_x^{\mathcal{T}g}[n,m]}{y_x^g[n,m]}\right)\right) \tag{26}$$

$$\hat{m}[n,m] = \mathrm{Round}\left(\frac{M}{2\pi}\mathrm{Im}\left(\frac{T_s y_x^{\mathcal{D}g}[n,m]}{y_x^g[n,m]}\right)\right) \tag{27}$$

and for the Levenberg-Marquardt reassignment we have

$$\tilde{n}[n,m] = n - \mathrm{Round}\left(\frac{1}{\Lambda}\left(T_s^{-1}\frac{\partial \Psi_x^g}{\partial\omega}\right)\left(1+\mu-\frac{\partial^2\Psi_x^g}{\partial t\partial\omega}\right) - \frac{1}{\Lambda}\left(T_s^{-2}\frac{\partial^2\Psi_x^g}{\partial\omega^2}\right)\left(\frac{2\pi m}{M} - T_s\frac{\partial\Psi_x^g}{\partial t}\right)\right) \tag{28}$$

$$\tilde{m}[n,m] = m - \mathrm{Round}\left(\frac{M}{2\pi\Lambda}\left(T_s^{-1}\frac{\partial\Psi_x^g}{\partial\omega}\right)\left(T_s^2\frac{\partial^2\Psi_x^g}{\partial t^2}\right) + \frac{1}{\Lambda}\left(\mu+\frac{\partial^2\Psi_x^g}{\partial t\partial\omega}\right)\left(m - \frac{MT_s}{2\pi}\frac{\partial\Psi_x^g}{\partial t}\right)\right) \tag{29}$$

with $\Lambda = \left(\mu + \frac{\partial^2\Psi_x^g}{\partial t\partial\omega}\right)\left(\mu+1-\frac{\partial^2\Psi_x^g}{\partial t\partial\omega}\right) + \left(T_s^2\frac{\partial^2\Psi_x^g}{\partial t^2}\right)\left(T_s^{-2}\frac{\partial^2\Psi_x^g}{\partial\omega^2}\right)$

Thus, the resulting discrete-time recursive reassigned spectrogram can be expressed as

$$\mathrm{R}_k[n,m] = \sum_{n'\in\mathbb{Z}}\sum_{m'=0}^{M-1} \left|y_k[n',m']\right|^2 \delta\left[n-\hat{n}[n',m']\right] \delta\left[m-\hat{m}[n',m']\right] \tag{30}$$

where $\delta[n]$ is the Kronecker delta and $(\hat{n},\hat{m})$ can be replaced by $(\tilde{n},\tilde{m})$ to obtain the Levenberg-Marquardt recursive reassigned spectrogram. The recursive synchrosqueezed STFT can be obtained as

$$\mathrm{Sy}_{k[n,m]} = \sum_{m'=0}^{M-1} y_{k[n,m']}\,\mathbf{e}^{-\frac{2j\pi m' n_0}{M}}\,\delta\left[m-\hat{m}_{[n,m']}\right] \tag{31}$$

where $n_0 = t_0/T_s$ can be chosen as the time instant when the maximum of h_k is reached (*i.e.* $n_0 = (k-1)L$). Thus, x can be recovered from $\mathrm{Sy}_k[n,m]$ by

$$\hat{x}[n-n_0] = \frac{1}{MT_s h_k(n_0 T_s)}\sum_{m=0}^{M-1}\mathrm{Sy}_k[n,m]. \tag{32}$$

As the proposed reassignment and synchrosqueezing methods are implemented not by FFTs but by filters banks, the computational cost can be reduced by reducing the range of the computed frequency m to the expected frequency support of the analyzed signal. When using the synchrosqueezed STFT, this range reduction can also be used for mode retrieval or denoising, as proposed in [6]. All results presented in this section provide time-frequency analysis tools that are independent of the signal sampling rate.

4. EXPERIMENTAL RESULTS

Fig.1 compares the proposed recursive TFRs obtained for a 500 samples long multicomponent real signal made of two impulses, one sinusoid, one chirp and one sinusoidally modulated sinusoid. The animations included in the subfigures, available with Adobe Reader© [14], show the results obtained for M=300 and a Signal-to-Noise Ratio (SNR) varying from 45 dB down to 5 dB (obtained by addition of a white Gaussian noise), with different values for k, L and μ. These animations clearly illustrate the improvement of the signal components localization brought by the proposed TFRs. For the Levenberg-Marquardt approach, the damping parameter μ shall not be chosen too small. Since only its frequency localization is improved, the synchrosqueezed STFT does not improve the time localization of the impulses. However it allows signal reconstruction and modes separation. Table 1 shows the sensitivity to n_0, M and μ of the signal Reconstruction Quality Factor (RQF), defined as

$$\text{RQF} = 10\log_{10}\left(\frac{\sum_n |x[n]|^2}{\sum_n |x[n]-\hat{x}[n]|^2}\right) \tag{33}$$

(a)	n_0	8	18	26	**28**	30
	RQF (dB)	9.79	24.17	26.77	**26.82**	26.73
(b)	M	100	200	600	1000	**2400**
	RQF (dB)	20.56	24.90	29.48	30.50	**30.87**
(c)	μ	0.30	0.80	1.30	1.80	**2.30**
	RQF (dB)	20.83	27.28	29.68	30.35	**30.90**

Table 1. Signal RQF of the recursive synchrosqueezed STFT computed for $k=5$, $L=7$ at SNR$\,=45$ dB. Line (a), computed for M=300, shows that the best RQF is obtained for $n_0 = (k-1)L$, but decreasing n_0 only slightly decreases the RQF, while decreasing the signal reconstruction delay. Line (b), computed for n_0=28, shows that the RQF increases with M, but choosing $M = 200$ only decreases the RQF from 6 dB compared to $M = 2400$. Line (c), computed for n_0=28 and M=300, shows that using a Levenberg-Marquardt synchrosqueezed STFT with values of μ larger than 0.7 provides a better RQF than the classical synchrosqueezed STFT (going to the RQF of the STFT, see Eq. (14), equal to 35.56 dB), while smaller values of μ provide a better signal localization.

5. CONCLUSION

We proposed a recursive implementation of the Levenberg-Marquardt reassignment and of the synchrosqueezing. Both are based on the use of causal recursive filters. Thanks to the Levenberg-Marquardt algorithm, these methods can allow a user to adjust the strength of the signal localization in the time-frequency plane while allowing a signal reconstruction. Future works will consist in proposing related real-world data analysis applications and to extend this approach to second-order synchrosqueezing [15]. A MATLAB implementation of the proposed methods can be found on-line at [16].

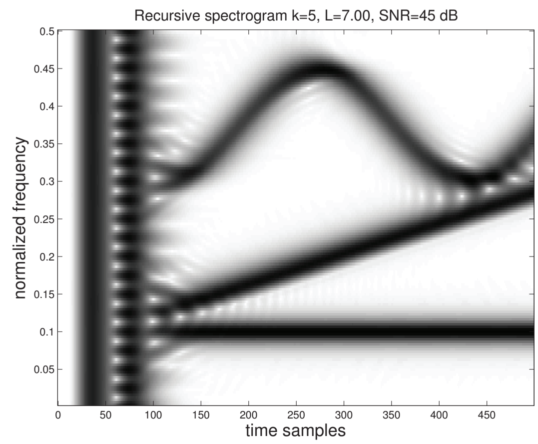

(a) spectrograms obtained for several k and SNR values.

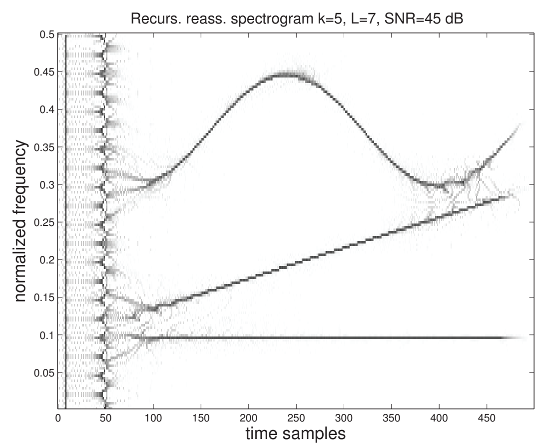

(b) classical and LM reassigned spectrograms.

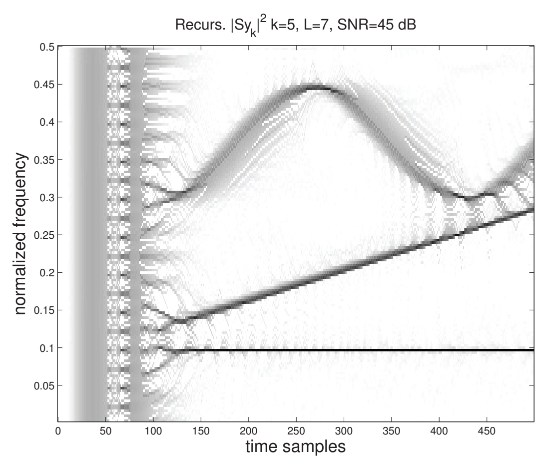

(c) squared modulus of classical- and LM-synchrosqueezed STFTs.

Fig. 1. Recursive time-frequency energy distributions of a multicomponent signal. All figures use a linear gray scale and show $\text{TFR}[n,m]^\alpha$ with α=0.4 for the spectrogram and reassigned spectrogram, and α=0.25 for the synchrosqueezing.

6. REFERENCES

[1] K. Kodera, C. de Villedary, and R. Gendrin, "A new method for the numerical analysis of non-stationary signals," *Physics of the Earth and Planetary Interiors*, vol. 12, pp. 142–150, 1976.

[2] F. Auger and P. Flandrin, "Improving the readibility of time-frequency and time-scale representations by the reassignment method," *IEEE Trans. Signal Process.*, vol. 43, no. 5, pp. 1068–1089, May 1995.

[3] F. Auger, E. Chassande-Mottin, and P. Flandrin, "Making reassignment adjustable: The Levenberg-Marquardt approach," in *Proc. IEEE ICASSP'12*, March 2012, pp. 3889–3892.

[4] I. Daubechies and S. Maes, "A nonlinear squeezing of the continuous wavelet transform based on auditory nerve models," *Wavelets in Medecine and Biology*, pp. 527–546, 1996.

[5] F. Auger, P. Flandrin, Y-T Lin, S. McLaughlin, Meignen S., T. Oberlin, and H-T. Wu, "Time-frequency reassignment and synchrosqueezing: an overview," *IEEE Signal Process. Mag.*, vol. 30, no. 6, pp. 32–41, November 2013.

[6] S. Meignen, T. Oberlin, and S. McLaughlin, "A new algorithm for multicomponent signals analysis based on synchrosqueezing: With an application to signal sampling and denoising," *IEEE Signal Process. Lett.*, vol. 60, no. 11, pp. 5787–5798, Nov 2012.

[7] Y. Guo, X. Fang, and X. Chen, "A new improved synchrosqueezing transform based on adaptive short time Fourier transform," in *Proc. IEEE Far East Forum on Nondestructive Evaluation/Testing (FENDT)*, June 2014, pp. 329–334.

[8] J. Thakur and H.-T. Wu, "Synchrosqueezing based recovery of instantaneous frequency from nonuniform samples," *SIAM J. Math. Anal.*, vol. 43, no. 5, pp. 20782095, 2011.

[9] G.K. Nilsen, "Recursive time-frequency reassignment," *IEEE Trans. Signal Process.*, vol. 57, no. 8, pp. 3283–3287, Aug 2009.

[10] Q.-H. Jo, J.-H. Chang, J.W. Shin, and N.S. Kim, "Statistical model-based voice activity detection using support vector machine," *IET Signal Processing*, vol. 3, no. 3, pp. 205–210, 2009.

[11] J. Huillery, F. Millioz, and N. Martin, "On the description of spectrogram probabilities with a chi-squared law," *IEEE Trans. Signal Process.*, vol. 56, no. 6, pp. 2249–2258, June 2008.

[12] F. Auger, E. Chassande-Mottin, and P. Flandrin, "On phase-magnitude relationships in the short-time Fourier transform," *IEEE Signal Process. Lett.*, vol. 19, no. 5, pp. 267–270, May 2012.

[13] L.B. Jackson, "A correction to impulse invariance," *IEEE Signal Process. Lett.*, vol. 7, no. 10, pp. 237–275, October 2000.

[14] "Adobe Reader," `https://get.adobe.com/reader/`, Accessed: January 14, 2016.

[15] T. Oberlin, S. Meignen, and V. Perrier, "Second-order synchrosqueezing transform or invertible reassignment? towards ideal time-frequency representations," *IEEE Trans. Signal Process.*, vol. 63, no. 5, pp. 1335–1344, March 2015.

[16] "ASTRES project MATLAB resources," `http://www.ens-lyon.fr/PHYSIQUE/Equipe3/ANR_ASTRES/resources.html`, Accessed: January 14, 2016.